Liquation Cracking in Full Penetration Al-Si Welds

Unlike wrought aluminum alloys, the widely used high-Si, Al-Si casting alloys can completely backfill and heal liquation cracks in welds regardless of the filler metal used

BY G. CAO AND S. KOU

ABSTRACT. Liquation cracking was investigated in the partially melted zone (PMZ) in welds of Al-Si alloys, which are widely used as casting alloys and often rich in Si to ensure good castability. Alloy A357 (Al-7Si) was selected as an example for studying liquation cracking in castings repaired or joined by welding. The crack susceptibility was evaluated by the circular-patch test, and full penetration, gas metal arc welds made with filler metals 1100 (Al), 4043 (Al-5Si), 4047 (Al-12Si), and 5356 (Al-5Mg). The PMZ consisted of α dendrites and interdendritic eutectic similar to the base metal, and the interdendritic eutectic coarsened and became α and Si particles in the heat-affected zone(HAZ). Liquation cracking was significant with filler metals 1100 and 5356 but slight with filler metals 4043 and 4047. Based on the multicomponent Scheil model and including as many as 10 different elements, curves of temperature (T) vs. fraction solid (f_S) were calculated for the weld metal and the PMZ, which are competing with each other in increasing f_S, and hence crack resistance. It is proposed that liquation cracking can occur if the weld-metal f_S > the PMZ f_S during the last 40°C of PMZ solidification before f_S reaches 0.99 (beyond which there is too little grain-boundary liquid to cause liquation cracking). It was found that in welds with significant liquation cracking (filler metals 1100 and 5356), the weld-metal f_S was significantly higher in the temperature range, while in welds with slight liquation cracking (filler metals 4043 and 4047), it was only slightly higher. In all welds, liquation cracks were completely backfilled and healed, instead of open as in full penetration welds of wrought aluminum alloys, such as Alloys 2219 and 6061. The T-f_S curves showed that, as compared to Alloys 2219 and 6061, Alloy A357 had a much higher fraction liquid ($1 - f_S$) for backfilling before PMZ solidification was essentially over ($f_S = 0.99$). The T-f_S curves were also calculated for two other high-Si, Al-Si casting alloys, A356 and 359, and the fraction liquid was high before PMZ solidification was essentially over, thus suggesting a strong tendency for backfilling and healing.

G. CAO and S. KOU are respectively a Graduate Student and a Professor in the Department of Materials Science and Engineering, University of Wisconsin, Madison, Wisc.

Introduction

The partially melted zone (PMZ) is a region immediately outside the weld metal where liquation occurs during welding because of overheating above the eutectic temperature (or the solidus temperature if the workpiece is completely solutionized before welding) (Ref. 1).

Liquation cracking in the welds of wrought aluminum alloys, including 2000- and 6000-series alloys, has been investigated by many investigators (Refs. 2–22). Liquation cracks in full penetration welds of wrought aluminum alloys are typically open instead of backfilled and healed (Refs. 2–5, 19, 20). Unlike Al-Cu and Al-Mg-Si welds, liquation cracking in welds on Al-Si castings has seldom been studied although Al-Si alloys are widely used in casting.

Gittos and Scott (Ref. 5) studied liquation cracking in full penetration Al-Mg-Si welds made in Alloy 6082. They proposed a liquation-cracking theory based on the equilibrium solidus temperature (T_S), that is, liquation cracking occurs when the weld-metal solidus temperature is higher than the base metal solidus temperature. While this theory helps understand liquation cracking in Alloy 6082, the use of T_S, unfortunately, prevents nonequilibrium solidification, which prevails in welding, from being considered. Contrary to Gittos and Scott, Miyazaki et al. (Ref. 9) found that in partial-penetration Al-Mg-Si welds made in Alloy 6061, the weld-metal solidus temperature was lower than the base-metal solidus temperature whether liquation cracking occurred or not.

Huang and Kou (Ref. 19) studied liquation cracking in full penetration Al-Cu welds made in Alloy 2219. A necessary condition for liquation cracking in full penetration Al-Cu welds was proposed. That is, the weld metal must be higher in fraction solid than the PMZ throughout PMZ solidification. This is because the solidifying weld metal contracts and pulls the solidifying PMZ. Huang and Kou (Ref. 20) also studied liquation cracking in full penetration Al-Mg-Si welds in Alloy 6061. A necessary condition for liquation cracking in full penetration Al-Mg-Si welds was also proposed. That is, the weld metal must be higher in fraction solid than the PMZ during part of PMZ terminal solidification. Since either condition is based on the fraction solid, nonequilibrium solidification can be considered, either through the basic Scheil model or more advanced solidification models that can predict T-f_S curves more accurately than the Scheil model. In the case of Alloy 6061 (Ref. 20), the following six elements were included in the calculation of T-f_S curves: Al, Cu, Mg, Mn, Si, and Zn. Trace elements Cr, Ti, and Fe were neglected.

Additional conditions required for liquation cracking to occur in any full penetration welds include (Ref. 20): 1) a significant tendency for the workpiece to contract during solidification, 2) significant restraint to keep the workpiece from contracting freely, 3) significant liquation

KEY WORDS

Aluminum Alloys
Backfilling
Fraction Solid
Heat-Affected Zone
Liquation Cracking
Partially Melted Zone
Scheil Model

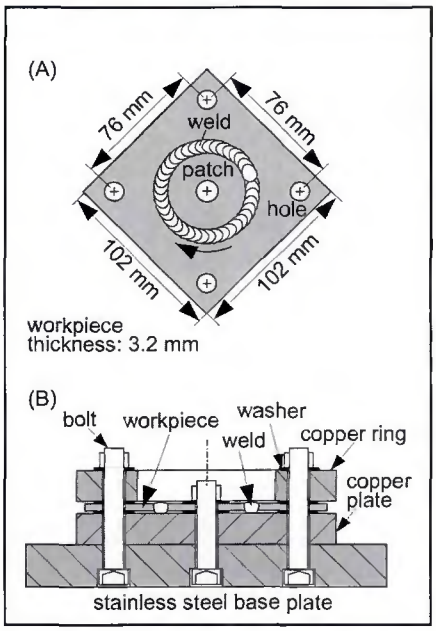

Fig. 1 — Circular patch test. A — Top view of workpiece; B — vertical cross-sectional view of apparatus.

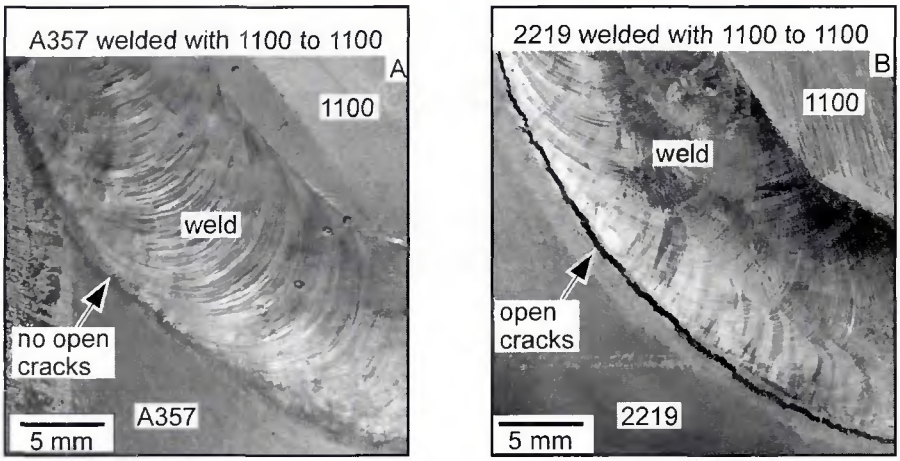

Fig. 2 — Macrographs of circular patch welds and liquation cracks. A — Alloy A357 welded with filler metal 1100 to 1100 patch; B — Alloy 2219 welded with filler metal 1100 to 1100 patch.

Table 1 — Compositions of the Workpiece and Filler Metal (wt-%)

	Si	Cu	Fe	Mg	Mn	Ti	Zn	Al
				Sheets				
1100	0.78	0.10	—	—	0.01	—	0.01	bal.
A357	6.92	0.053	—	0.56	0.023	—	—	bal.
				Filler Metals				
1100	0.08	0.08	0.52	—	0.01	—	0.02	bal.
4043	5.20	0.30	0.80	0.05	0.05	0.20	0.10	bal.
4047	11.60	0.030	—	0.02	—	—	—	bal.
5356	—	—	—	5.00	0.12	—	—	bal.

to weaken the PMZ, and 4) no solidification cracking nearby to relax the strains in the PMZ. Liquation cracking is not likely to occur in full penetration welds if the weld metal has a lower fraction solid than the PMZ throughout PMZ solidification.

Regarding the first additional condition, the workpiece contracts during welding mainly because of solidification shrinkage and thermal contraction of the weld metal. The solidification shrinkage of aluminum is as high as 6.6% (Ref. 23), and the thermal expansion coefficient of aluminum is roughly twice that of iron-based alloys.

Partial penetration aluminum welds made with gas metal arc welding and Ar shielding often exhibit capillary penetration. Huang and Kou (Ref. 18) found that the weld root is not smooth along the welding direction but wavy with liquation cracks in the areas between waves. A mechanism that takes into account penetration oscillation was proposed to explain liquation cracking in such welds.

Unlike liquation cracking in wrought aluminum alloys, liquation cracking in casting aluminum alloys has seldom been studied. Welding is routinely used for repairing casting defects in aluminum alloys. Solidification cracks, cold shuts, and gas holes in aluminum castings are often closed by repair welding with a filler metal. Sometimes, an aluminum casting needs to be welded to a wrought aluminum alloy. It is essential to ensure that welding does not induce liquation cracking. Aluminum alloys with silicon as a major alloying ingredient are by far the most important commercial aluminum casting alloys, primarily because of their superior castability (Ref. 24). Such alloys are known to have good fluidity and high resistance to solidification cracking. The purpose of the present study was to investigate liquation cracking in welds on Al-Si castings.

Experimental Procedure

The circular-patch test (Ref. 25) was used to evaluate the susceptibility to liquation cracking. The apparatus is shown in Fig. 1. The workpiece was highly restrained (by being bolted down to a thick stainless steel plate) in order to prevent it from contracting freely during welding. This allowed liquation cracking to occur during welding and the crack susceptibility to be evaluated. A similar design was used by Nelson et al. (Ref. 26) for assessing solidification cracking in steel welds.

An Alloy A357 billet of 102 mm diameter by 300 mm length prepared by casting was used. Squares 102 × 102 × 5 mm were cut from the billet and milled down from 5 to 3.2 mm for use as the workpiece. Circular patches were also prepared from the same billet with a square edge.

As shown in Fig. 1, the workpiece of Alloy A357 was sandwiched between a copper plate at the bottom and a copper ring at the top. The copper plate was 152 × 152 × 19 mm. The copper ring was 19 mm thick, with an 83-mm inside diameter, and having dimensions of 152 × 152 mm on the outside. The workpiece, together with the copper plate and the copper ring were bolted down tightly to a 25.4 mm-thick stainless steel base plate 203 × 203 mm. The bolts, located at holes at the center and each corner of the workpiece, were tightened with a torque wrench to the same torque of 47.5 m N to ensure consistent restraint on the workpiece. The center hole was 12.7 mm diameter and the corner holes 11.1 mm. The workpiece was actually separated from the copper plate and ring with 1.6-mm-thick steel washers having a 12.2-mm inside diameter and 23.5-mm outside diameter. Without the washers, it was difficult to make full penetration welds because of the heat-sink effect of the copper ring.

Four filler metals were used, 1100, 4043, 4047 and 5356, all 1.2 mm in diameter. In one and only one experiment, a circular patch of base Alloy 1100 was used in order to lower the weld metal Si content as much as possible, by using filler metal 1100 for welding. In all experiments, the patch had a 57.2-mm diameter, and the gap of the square butt joint between the outer piece and the patch was about 0.25

mm. The compositions of Alloy A357, Alloy 1100, and filler metals 1100, 4043, 4047, and 5356 are all shown in Table 1.

The apparatus was mounted horizontally on a welding positioner to allow rotation under a stationary gas metal arc welding (GMAW) gun. Gas metal arc welding was conducted with direct current electrode positive (DCEP) using a constant voltage power supply, and the welding parameters were 4.2 mm/s welding speed (based on a 1.6 rpm rotation speed and a 5.1 cm diameter), 22 V, 140 A average current, and Ar shielding. The filler metal, 1.2 mm in diameter, was positioned at 25.4 mm from the center of the workpiece. The wire feed speed was 93 mm/s for 1100, 4043, and 4047, but 114 mm/s for 5356 in order to keep the welding current close to 140 A. The distance between the contact tip and workpiece was about 25.4 mm, and the welding gun was perpendicular to the workpiece.

The resultant welds were cut, polished, and etched with a solution of 0.5 vol-% HF in water for microstructural examination by optical microscopy. The transverse cross-sectional area of each weld was determined with a digital camera and a computer using commercial software.

It has been shown that the composition of a single-pass GMA aluminum weld is essentially uniform (Ref. 27). The Lorenz force, surface-tension gradients, and droplet impingement help mix the filler metal with the melted base metal (Ref. 1). As such, the concentration of an alloying element E in the weld metal was calculated from those in the base metals and the filler metal using the following equation

$$\%\ \text{element}\ E\ \text{in weld metal} = [(\%\ E\ \text{in base metal}\ A) \times a + (\%\ E\ \text{in base metal}\ B) \times b + (\%\ E\ \text{in filler metal}\ C) \times c] / (a + b + c) \quad (1)$$

where a, b, and c are the areas in the weld transverse cross section that represent contributions from the base metal A (the outer piece), base metal B (the patch test), and filler metal C, respectively. They were determined from the area and location of the transverse cross section of the weld.

Results and Discussion

For convenience, all welds are identified by two numbers, the first referring to the workpiece and the second the filler metal. For instance, Weld A357/4047 refers to the weld made in Alloy A357 with a filler metal of Alloy 4047. There were two welds made in Alloy A357 with filler 1100, that is, A357/1100A and A357/1100. They were made with and without an 1100 circular patch, respectively. The measured

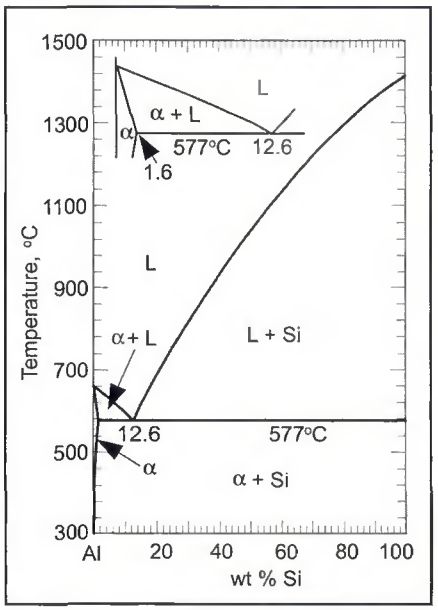

Fig. 3 — Binary Al-Si phase diagram (Ref. 28).

dilution ratios of the welds are shown in Table 2. The weld metal compositions, calculated based on the dilution ratios and the compositions of the workpiece and the filler metals, are also shown in Table 2.

The experimental results will be compared with previous studies involving wrought aluminum Alloys 2219 and 6061 (Refs. 19, 20).

Macrographs of Welds

Figure 2A shows the macrograph of Weld A357/1100A, that is, Alloy A357 welded to an Alloy 1100 patch with filler metal 1100. No open liquation cracks were visible. For comparison with a wrought alloy weld made in a similar way, weld 2219/1100A, that is, Alloy 2219 welded to an Alloy 1100 patch with filler metal 1100 (Ref. 19), is shown in Fig. 2B. Open liquation cracks are evident along the outer edge of the weld.

All other welds made in Alloy A357 had a macrograph similar to that shown in Fig. 2A and showed no open cracks.

Microstructures of Base Metal and HAZ

For convenience of discussion, the binary Al-Si phase diagram is shown in Fig. 3 (Ref. 28). As shown, Alloy A357, which is approximately a binary Al-6.9Si alloy, is hypoeutectic and its as-cast microstructure should consist of an Al-rich α phase and an Al-Si eutectic of approximately Al-12.6Si.

Figure 4A shows a typical microstructure of the base metal of Alloy A357. It consists of light-etching equiaxed α dendrites and dark-etching interdendritic Al-Si eutectic. Figure 4B shows a typical microstructure of the heat-affected zone (HAZ). The interdendritic Al-Si eutectic in the HAZ was heated to just below the eutectic temperature, causing it to coarsen and become α aluminum and Si particles, as shown in the enlarged HAZ micrograph in Fig. 4C.

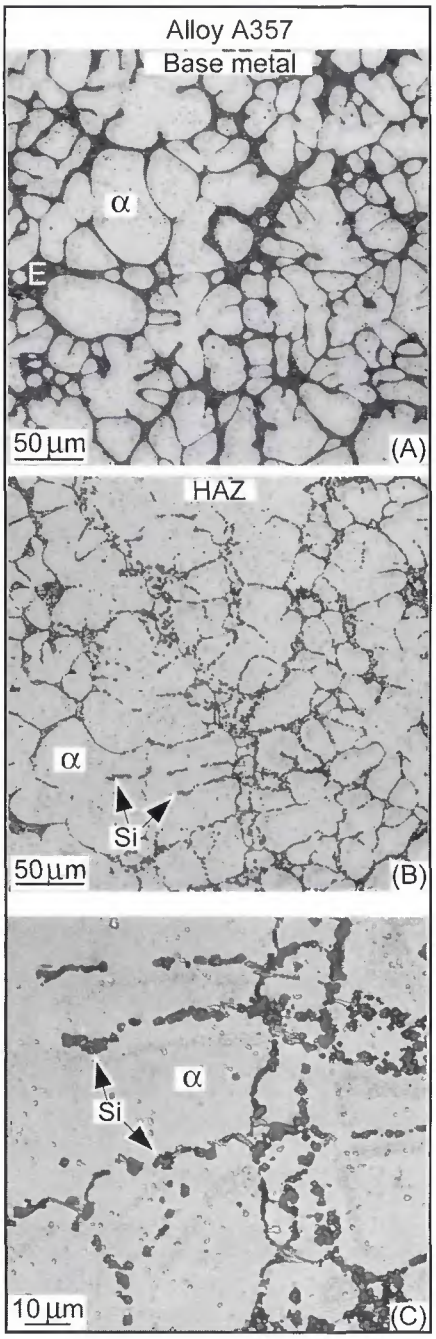

Fig. 4 — Typical microstructure of Alloy A357. A — Base metal; B — heat-affected zone (HAZ); C — HAZ enlarged. α, E, and Si denote aluminum-rich phase, interdendritic eutectic, and Si-rich particles, respectively.

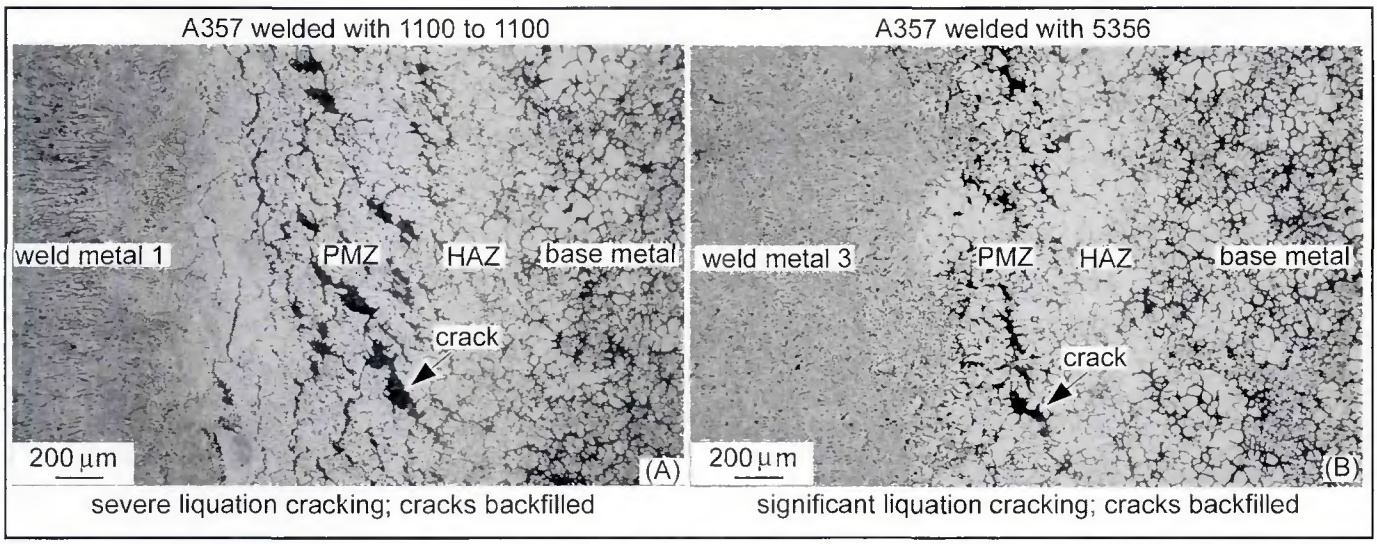

Fig. 5 — Overall weld microstructure. A — Alloy A357 welded with filler metal 1100 to 1100 patch; B — Alloy A357 welded with filler metal 5356. PMZ: partially melted zone; HAZ: heat-affected zone.

Table 2 — Weld Metal Dilution Ratios and Compositions (wt-%) Calculated Based on Equation 1

Weld (alloy/filler metal)	Dilution ratio	Si	Cu	Fe	Mg	Mn	Ti	Zn	Al
A357/1100A (weld metal 1)	13.0% from A357 47.9% from 1100 patch	1.30	0.086	0.20	0.073	0.012	—	0.013	balance
A357/1100 (weld metal 2)	63.2% from A357	4.41	0.063	0.19	0.35	0.018	—	0.007	balance
A357/5356 (weld metal 3)	59.3% from A357	4.10	0.031	—	2.37	0.062	—	—	balance
A357/4043 (weld metal 4)	64.6% from A357	6.31	0.140	0.28	0.38	0.033	0.071	0.035	balance
A357/4047 (weld metal 5)	65.0% from A357	8.56	0.045	—	0.37	0.015	—	—	balance

Overall Weld Microstructure

Figure 5A shows the overall micrograph of Weld A357/1100A covering from the weld metal to the base metal (Alloy A357). Liquation cracking was severe in the PMZ. However, the cracks appeared backfilled and healed. (This is shown more clearly in the enlarged micrograph in Fig. 6B.) This explains the lack of open cracks in the weld macrograph — Fig. 2A.

Figure 5B shows a similar micrograph of Weld A357/5356, that is, Alloy A357 welded with filler metal 5356. Liquation cracking was significant though not as severe as that in Weld A357/1100A — Fig. 5A. Again, the cracks appeared backfilled and healed. (This is shown more clearly in the enlarged micrograph in Fig. 8B.)

The overall micrographs of other welds are not shown here; however, Weld A357/1100 was similar to that of Weld A357/5356 (Fig. 5B) and also exhibited significant liquation cracking. Welds A357/4043 and A357/4047 had much less liquation cracking. In fact, liquation cracking in these welds was almost negligible.

Calculation of Temperature vs. Fraction Solid

In order to better understand the interaction between the weld metal and the PMZ during welding, the T-f_S (temperature vs. fraction solid) curves were calculated for the weld metal and the PMZ. A computer code *Pandat* was used, which is a software package for calculating multicomponent phase diagrams, solidification paths, and thermodynamic properties (Ref. 29). *PanAluminum* was also used, which is a thermodynamic database for aluminum alloys based on the experimental data of thermodynamic properties and phase equilibria (Ref. 30). The software and the database have been tested extensively against binary and multicomponent aluminum alloys (Refs. 31–47).

The database, *PanAluminum*, that was used consisted of 16 elements, which included all the following 10 elements in Tables 1–3: Al, Si, Cr, Cu, Fe, Mg, Mn, Ti, Zr, and Zn. The Scheil model for multicomponent alloys was used as an approximation, but with a temperature-dependent equilibrium partition ratio (k) and liquidus slope (m_L). If necessary, more advanced solidification models can be used to calculate the fraction solid more accurately than the Scheil model.

Welds Made with Filler Metal 1100

The micrographs and T-f_S curves of the weld metal and PMZ of Weld A357/1100A are shown in Fig. 6. The weld metal dendritic structure (Fig. 6A) is very different from the base metal dendritic structure (Fig. 4A) though both consisted of α dendrites and interdendritic eutectic. Severe liquation cracking is evident in the PMZ (Fig. 6B), suggesting that the solidifying and contracting weld metal pulled and tore the PMZ while the PMZ was solidifying. For this to occur, the solidifying weld

metal must be much more crack resistant than the solidifying PMZ.

The T-f_S curves (Fig. 6C) of the weld metal and the PMZ of Weld A357/1100A were calculated based on their compositions shown in Tables 1 and 2. The weld metal and the PMZ were essentially binary alloys of compositions Al-1.30Si and Al-6.92Si, respectively. The primary Al phase (α) starts to form from the liquid at the beginning of a T-f_S curve ($f_S = 0$). An arrest appears in a T-f_S curve when a secondary solid phase also starts to form from the liquid, that is, when the liquidus slope changes due to intersection with a line of two-fold saturation, such as a eutectic valley. For instance, in the curve for the PMZ of Alloy A357, the Si-rich phase starts to form at the first arrest at 573°C and Mg_2Si starts to form at the second arrest at 555°C. It is assumed that the secondary phase will nucleate as soon as such a valley is reached, that is, without significant undercooling.

Experimental data show that the strength (Refs. 23, 48–51) of a semisolid aluminum alloy increases with increasing fraction solid (decreasing temperature). During welding, the solidifying weld metal and the solidifying PMZ are connected to each other (at the fusion boundary) and under the tensile strains induced by solidification shrinkage and thermal contraction. Thus, the one with a higher fraction solid is likely to be more crack resistant (stronger) under tension if, as an approximation, the secondary effect of the microstructure and grain size on the strength or resistance to cracking is neglected.

Flemings (Ref. 23) pointed out that the strength of a semisolid is very low until some given fraction of solid is reached, usually in the range of 0.2 to 0.4 (approximately 0.3). According to the T-f_S curve of Alloy A357 (Fig. 6C), by the time the PMZ cools to about 590°C, its fraction solid exceeds 0.3. PMZ solidification is essentially over ($f_S = 0.99$) when the temperature drops to about 550°C. With $f_S > 0.99$, there is not likely to be sufficient grain-boundary liquid to form continuous films to cause liquation cracking. Thus, it seems reasonable to focus on the last 40°C of solidification before f_S reaches 0.99, which in the case of A357 is the temperature range of 590–550°C. Incidentally, "terminal solidification" refers to the last portion of solidification — usually a temperature range much narrower than the solidification range itself. Since the 40°C temperature range is not much narrower than the 65°C solidification range (615–550°C, again, not counting the final 1% liquid) of Alloy A357, it is not called the terminal portion of solidification in the present study.

It is proposed that liquation cracking is likely to occur in the PMZ if, within a significant portion of its last 40°C of solidification before f_S reaches 0.99, the PMZ becomes significantly lower in fraction solid, and hence resistance to cracking, than the solidifying weld metal, which is contracting and straining the PMZ.

As indicated by the T-f_S curves (Fig. 6C), the weld metal becomes much higher in f_S, and hence crack resistance, than the PMZ in the shaded area within the temperature range 590–550°C (bracketed). This explains the presence of severe liquation cracking in the PMZ of Weld A357/1100A.

The PMZ microstructure (Fig. 6B) shows that liquation cracks appeared to be completely filled with eutectic. This suggests that sufficient liquid was present in the PMZ to backfill and heal the cracks when they were formed. According to the PMZ T-f_S curve (Fig. 6C), at about 575°C there still exists approximately 52% liquid in the PMZ even though the weld metal has reached about 90% solid.

In Weld A357/1100A, the region of the weld metal adjacent to the PMZ appeared to be depleted of eutectic, as evident from the right-half of the micrograph in Fig. 6A. This region is also visible in Fig. 5A. It is

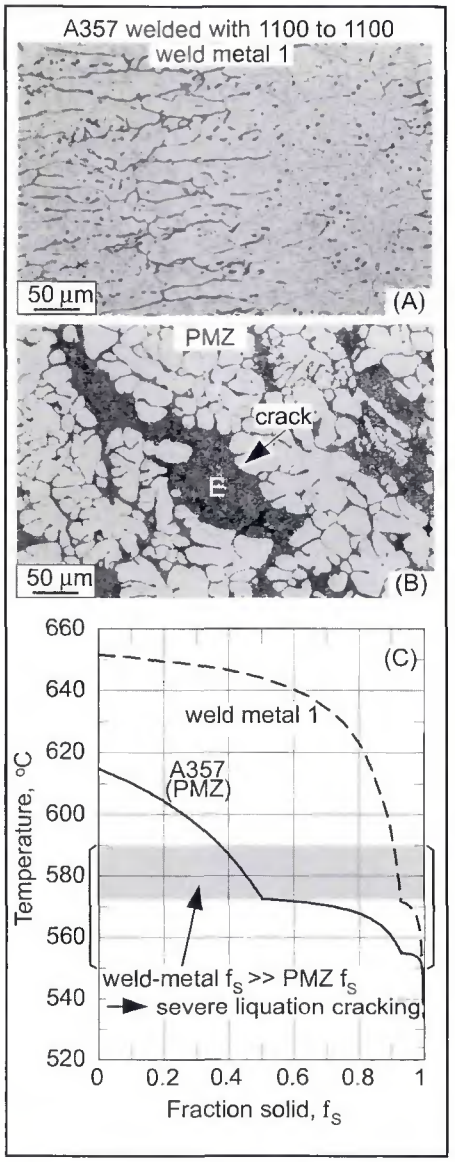

Fig. 6 — Alloy A357 welded with filler metal 1100 to 1100 patch. A — Weld metal; B — PMZ; C — T-f_S curves calculated using Pandat *of CompuTherm LLC (Ref. 29). Weld metal f_S far exceeds PMZ f_S in part (shaded) of the last 40°C of PMZ solidification before f_S=0.99 (bracketed).*

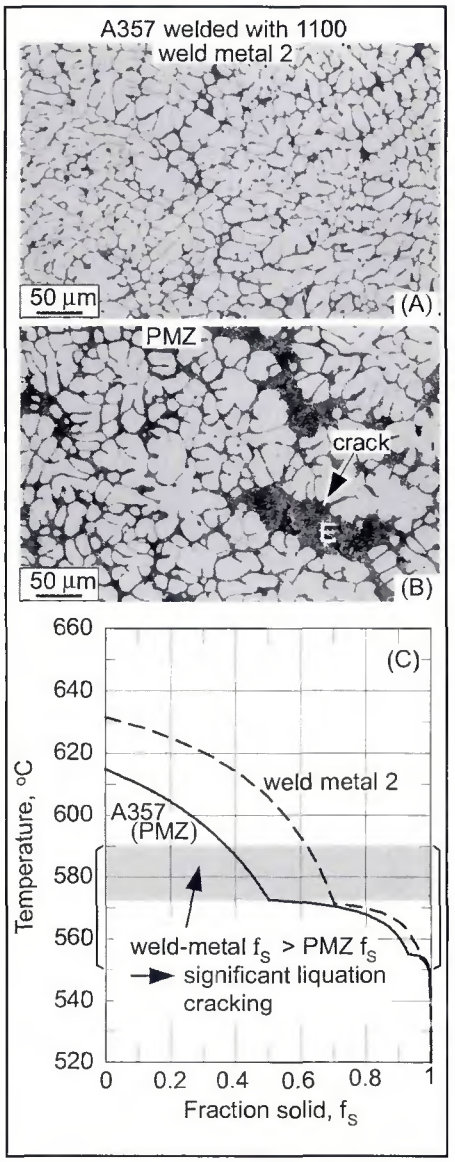

Fig. 7 — Alloy A357 welded with filler metal 1100. A — Weld metal; B — PMZ; C — T-f_S curves calculated using Pandat *of CompuTherm LLC (Ref. 29). Weld-metal f_S significantly exceeds PMZ f_S in part (shaded) of the last 40°C of PMZ solidification before f_S=0.99 (bracketed).*

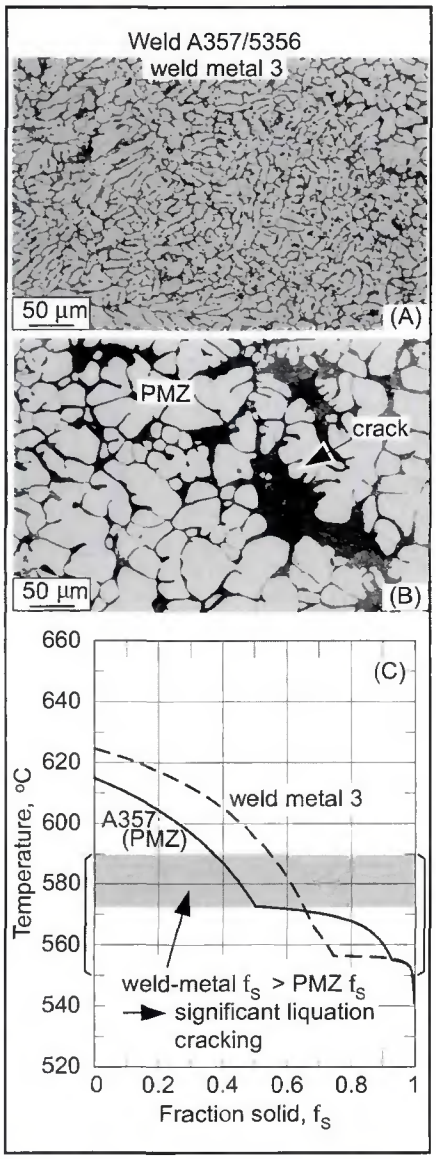

Fig. 8 — Alloy A357 welded with filler metal 5356. A — Weld metal; B — PMZ; C — T-f_S curves calculated using Pandat *of CompuTherm LLC (Ref. 29). Weld metal f_S significantly exceeds PMZ f_S in part (shaded) of the last 40°C of PMZ solidification before f_s=0.99 (bracketed).*

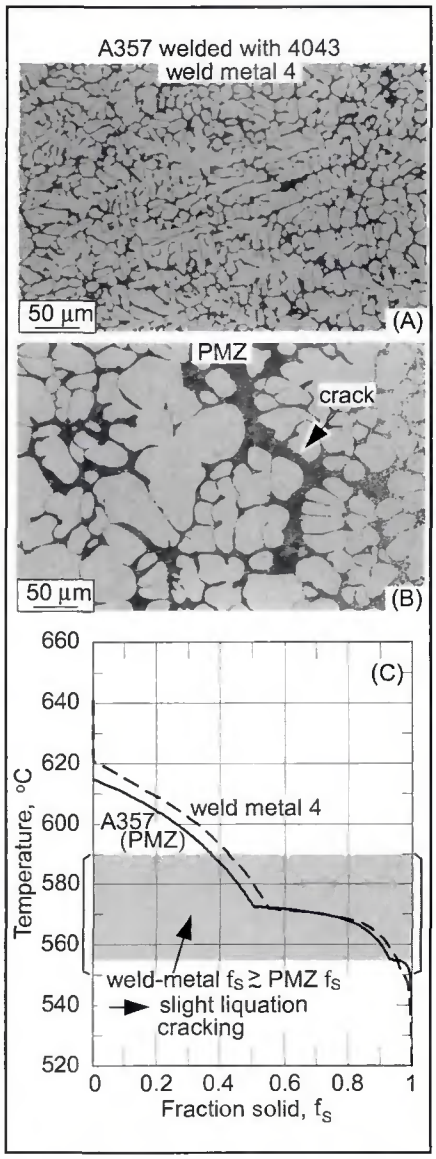

Fig. 9 — Alloy A357 welded with filler metal 4043. A — Weld metal; B — PMZ; C — T-f_S curves calculated using Pandat *of CompuTherm LLC (Ref. 29). Weld metal f_S slightly exceeds PMZ f_S in part (shaded) of the last 40°C of PMZ solidification before f_s=0.99 (bracketed).*

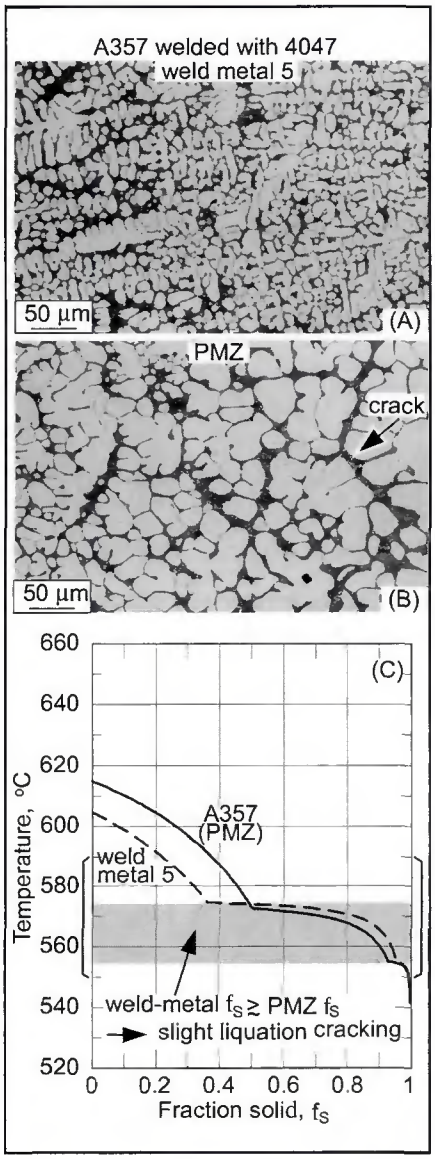

Fig. 10 — Alloy A357 welded with filler metal 4047. A — Weld metal; B — PMZ; C — T-f_S curves calculated using Pandat *of CompuTherm LLC (Ref. 29). Weld metal f_S slightly exceeds PMZ f_S in part (shaded) of the last 40°C of PMZ solidification before f_s=0.99 (bracketed).*

likely that the interdendritic liquid in the weld metal next to the PMZ flowed into the PMZ to compensate for the PMZ liquid that flowed to feed the cracks. This weld-metal interdendritic liquid was, in turn, compensated by the weld pool liquid near the pool boundary. Since the weld pool liquid was much leaner in solute than the weld metal interdendritic liquid, it caused a drop in the local average solute content of the weld metal (C_o), that is, averaged over local dendrites and interdendritic liquid. This caused the local fraction eutectic (f_E) to decrease as can be seen from the following form of the Scheil equation for binary alloys (Ref. 1)

$$f_E = \left(\frac{C_o}{C_E}\right)^{\frac{1}{1-k}} \qquad (2)$$

where k is the equilibrium partition ratio and C_E is the solute content of the eutectic.

The micrographs and T-f_S curves of the weld metal and PMZ of Weld A357/1100 are shown in Fig. 7. The weld metal dendritic structure (Fig. 7A) is much finer than the base metal dendritic structure (Fig. 4A), thus reflecting the much higher cooling rate in welding than in casting. Significant liquation cracking is evident in the PMZ (Fig. 7B), suggesting that the weld metal was significantly more crack resistant than the PMZ.

As shown by the calculated T-f_S curves (Fig. 7C), the weld metal is significantly higher in f_S, and hence crack resistance, than the PMZ in the shaded area within the temperature range 590–550°C. This explains the presence of significant liquation cracking in the PMZ. However, the difference between the weld metal f_S and the PMZ f_S is significantly less here than in the case of Weld A357/1100A — Fig.

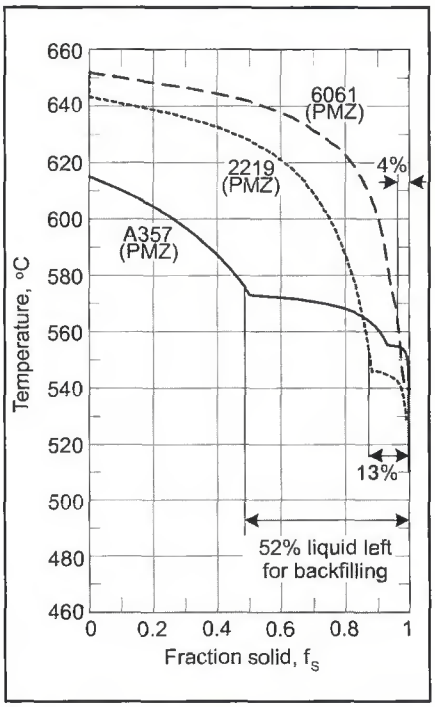

Fig. 11 — T-f_S curves explaining the much greater backfilling tendency of casting Alloy A357 than wrought Alloys 2219 and 6061. At about 25°C before solidification is essentially over (f_S = 0.99), much more liquid is left for backfilling in A357 (52%) than in 2219 (13%) and 6061 (4%). Curves calculated using Pandat *of CompuTherm LLC (Ref. 29).*

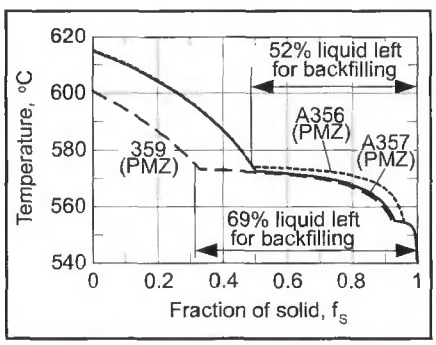

Fig. 12 — T-f_S curves explaining the strong backfilling tendency of three high-Si, Al-Si casting alloys. At about 25°C before solidification is essentially over (f_S = 0.99), much liquid is still available for backfilling in A356 (52%), A357 (52%), and 359 (69%). Curves calculated using Pandat *of CompuTherm LLC (Ref. 29).*

6C. This is because the difference between the weld metal composition (essentially Al-4.41Si) and the base metal composition (essentially Al-6.92Si) is less than in the case of Weld A357/1100A (essentially Al-1.30Si for the weld metal and Al-6.92Si for the base metal). Consequently, significant liquation cracking occurred in Weld A357/1100 (Fig. 7B) but not as severe as in Weld A357/1100A (Fig. 6B).

Table 3 — Nominal Compositions of Some Wrought and Casting Aluminum Alloys

	Si	Cr	Cu	Fe	Mg	Mn	Ti	Zn	Zr	Al
					Wrought Alloys (Refs. 19, 20)					
2219	0.08	—	6.30	0.12	—	0.33	0.03	0.01	0.12	bal.
6061	0.68	0.19	0.23	0.44	0.91	0.07	0.05	0.05	—	bal.
					Casting Alloys (Ref. 52)					
A356	7.0	—	0.053	—	0.35	0.023	—	—	—	bal.
359	9.0	—	0.053	—	0.56	0.023	—	—	—	bal.

Weld Made with Filler Metal 5356

The micrographs and T-f_S curves of the weld metal and PMZ of Weld A357/5356 are shown in Fig. 8. Again, the weld metal dendritic structure (Fig. 8A) was much finer than the base metal dendritic structure — Fig. 4A. Again, the PMZ dendritic structure shows significant liquation cracking (Fig. 8B), suggesting that the weld metal was significantly more crack resistant than the solidifying PMZ.

The calculated T-f_S curves (Fig. 8C) shows that the weld metal is significantly higher in f_S, and hence crack resistance, than the PMZ in the shaded area within the temperature range 590–550°C, which explains the presence of significant liquation cracking in the PMZ. The weld metal is lower in f_S than the PMZ from about 555 to 570°C but is significantly higher than the PMZ above approximately 575°C. According to the proposed model, this suggests that liquation cracking occurred in the PMZ above this temperature.

Welds Made with Filler Metals 4043 and 4047

The micrographs and T-f_S curves of the weld metal and PMZ of Weld A357/4043 are shown in Fig. 9. The weld metal dendritic structure (Fig. 9A) is again much finer than the base metal dendritic structure — Fig. 4A. The PMZ dendritic structure (Fig. 9B) exhibited a slight degree of liquation cracking. This suggests that the solidifying and contracting weld metal was slightly more crack resistant than the solidifying PMZ.

Within the temperature range 590–550°C (Fig. 9C), the weld metal can be slightly higher in f_S, and hence crack resistance, than the PMZ, although the difference in f_S is reversed below 555°C. The combination of this small difference in f_S and the ductile equiaxed-grain structure of the PMZ explains the slight liquation cracking in the PMZ of Weld A357/4043. As shown in Table 1, filler metal 4043 contained 0.2% Ti, and this caused Al_3Ti precipitation at the early stages of solidification, at approximately 641°C.

The micrographs and T-f_S curves of the weld metal and PMZ of Weld A357/4047 are shown in Fig. 10. The liquation cracking exhibited by this weld was very small and the PMZ microstructure (Fig. 10B) looked very similar to the base-metal microstructure — Fig. 4A. According to the calculated T-f_S curves (Fig. 10C), the weld metal is slightly higher in f_S, and hence crack resistance, than the PMZ from 575–555°C, which is within the temperature range 590–550°C. This small f_S difference, in conjunction with the ductile equiaxed-grain structure of the PMZ, explains the slight degree of liquation cracking in the PMZ of Weld A357/4047. Above about 575°C the weld metal is lower in f_S than the PMZ.

Casting Alloy A357 vs. Wrought Alloys 2219 and 6061

As mentioned previously, Huang and Kou (Ref. 19) reported open liquation cracks along the outer edge of the weld in wrought aluminum Alloy 2219 welded with filler metal 1100 to an 1100 patch (Fig. 2B) and 6061 welded with filler metal 5356 (Ref. 20). In contrast, liquation cracks in casting aluminum Alloy A357 welded with filler metal 1100 to an 1100 patch (Figs. 2A, 5A, and 6B) and welded with filler metal 5356 (Figs. 5B and 8B) were closed and healed by backfilling. In order to explain this striking difference, the T-f_S curves of Alloys 2219 and 6061 were also calculated based on their compositions shown in Table 3.

According to the calculated T-f_S curves shown in Fig. 11, the PMZ of Alloy A357 has as much as 52% liquid at 575°C, that is, 25°C before solidification is essentially over at 550°C (f_S = 0.99). The PMZ of Alloy 2219, on the other hand, has only 13% liquid at 554°C, that is, 25°C before solidification is essentially over at 529°C (f_S = 0.99). Thus, backfilling of PMZ cracks can be expected to be significantly more difficult in Alloy 2219 than in A357. As shown in Table 3, Alloy 2219 contained 0.12% Zr particles, which suggests that Al_3Zr particles are present prior to solidification.

As for Alloy 6061, the PMZ has as little as 4% liquid at 565°C, that is, 25°C before solidification is essentially over at 540°C (f_S = 0.99). As such, backfilling and healing of

PMZ cracks can be expected to be far more difficult in Alloy 6061 than in A357.

Other Si-rich Al-Si Casting Alloys

Two other popular Si-rich casting alloys, A356 and 359 (Ref. 52), were also studied based on their PMZ T-f_S curves. Theses curves are shown in Fig. 12. The curves were calculated based on the compositions shown in Table 3. The T-f_S curve of A356 is close to that of A357. This suggests that its tendency to backfill liquation cracks is expected to be essentially as high as Alloy A357. At 25°C before solidification is essentially over (f_S = 0.99), that is, at 575°C, there is still as much as 69% liquid available for backfilling in Alloy 359, as compared to 52% in Alloy A357. This suggests that Alloy 359 has an even stronger tendency to backfill liquation cracks than Alloy A357.

Hence, when welded with filler metals 1100 or 5356, Si-rich casting Alloys A356 and 359 are expected to be susceptible to liquation cracking but the cracks are likely to be healed by backfilling, as in the case of Alloy A357.

High-Si, Al-Si alloys containing more than 1% Cu can solidify over a much wider temperature range, that is, with solidification extending to a significantly lower temperature than those without Cu. Further studies are needed to evaluate the liquation cracking of these alloys.

Conclusions

The present study was conducted to investigate liquation cracking in full penetration Al-Si welds. Alloy A357 (Al-7Si) was selected because high-Si, Al-Si alloys are widely used as casting alloys due to their good fluidity and high resistance to solidification cracking. Liquation cracking can occur in such alloys when welding is used to close defects (such as solidification cracks, cold shuts, and gas holes) in castings or join castings to wrought aluminum alloys. In this study, the circular patch test was used to evaluate the liquation cracking susceptibility. Full penetration, gas-metal arc welds were made with filler metals 1100 (Al), 4043 (Al-5Si), 4047 (Al-12Si), and 5356 (Al-5Mg). Liquation cracking in the partially melted zone was examined experimentally and explained based on the calculated solid volume fraction established during solidification.

The conclusions derived from casting Alloy A357, which are believed to be also valid for high-Si, Al-Si casting Alloys A356 and 359, are as follows:

1) The partially melted zone (PMZ) in welds of high-Si, Al-Si casting alloys consists of α dendrites and interdendritic eutectic similar to the base metal. In the heat-affected zone, the interdendritic eutectic coarsens and becomes Al-rich α and Si particles upon heating to below the eutectic temperature.

2) Filler metals 1100 and 5356 are much more likely to cause liquation cracking in the PMZ of high-Si, Al-Si casting alloys than filler metals 4043 and 4047. This suggests the use of filler metals 4043 and 4047 for repairing castings of these alloys by welding.

3) Severe liquation cracking can occur when welding high-Si, Al-Si casting alloys to Alloy 1100, especially when using filler metal 1100. This suggests that welding castings of these alloys to Alloy 1100 should be avoided. If this is not possible, filler metal 4047 should be used instead of filler metal 1100.

4) The tendency for liquation cracking to occur in the PMZ of high-Si, Al-Si casting alloys increases with decreasing Si content in a binary Al-Si weld metal. In other words, the tendency for liquation cracking increases in the order of filler metals 4047, 4043, and 1100. It increases further when welding these alloys to Alloy 1100 with filler metal 1100 because of a further decrease in the weld metal's Si content.

5) It is proposed that liquation cracking is likely to occur in the PMZ if, within the last 40°C of solidification before f_S reaches 0.99, the PMZ becomes significantly lower in f_S, and hence resistance to cracking, than the solidifying weld metal, which contracts and strains the PMZ. For Alloy A357, this temperature range is 590–550°C.

6) Curves of temperature (T) vs. fraction solid (f_S) have been calculated for both the PMZ (same as the base metal) and the weld metal of high-Si, Al-Si casting alloys using the multicomponent Scheil model of solidification that included the following ten elements: Al, Si, Cr, Cu, Fe, Mg, Mn, Ti, Zr, and Zn.

7) With filler metals 1100 and 5356, the weld metal that is solidifying, contracting, and straining the solidifying PMZ can be significantly higher in f_S (and hence crack resistance) than the PMZ within the temperature range of 590–550°C. This explains the significant liquation cracking observed in high-Si, Al-Si casting alloys welded with filler metals 1100 and 5356.

8) When welding high-Si, Al-Si casting alloys to Alloy 1100 with filler metal 1100, the weld metal can be much higher in f_S (and hence crack resistance) than the PMZ f_S within the temperature range of 590– 550°C. This explains the severe liquation cracking in these welds.

9) With filler metals 4043 and 4047, the weld metal can be only slightly higher in f_S (and hence crack resistance) than the PMZ within the temperature range of 590– 550°C. The combination of this small difference in f_S and the ductile equiaxed-grain structure of the PMZ explains the slight liquation cracking in high-Si, Al-Si casting alloys welded with filler metals 4043 and 4047.

10) Liquation cracks in full penetration welds of high-Si, Al-Si casting alloys tend to be completely backfilled and thus healed — contrary to the open liquation cracks in full penetration welds of wrought aluminum alloys such as 2219 welded with filler metal 1100 and 6061 welded with filler metal 5356. Furthermore, complete backfilling and healing can occur in welds of high-Si, Al-Si alloys regardless of the filler metal used.

11) T-f_S curves show that before PMZ solidification is essentially over (f_S = 0.99), the fraction liquid (1 – f_S) is much higher in high-Si, Al-Si casting alloys than in Alloys 2219 and 6061. This suggests that much more liquid is available for backfilling and healing of liquation cracks in high-Si, Al-Si casting alloys. This explains why open liquation cracks are present in alloys 2219 and 6061, but not in high-Si, Al-Si casting alloys.

Acknowledgments

This work was supported by National Science Foundation under Grant No. DMR-0098776. The authors would like to thank Justin Heimsch of Madison-Kipp Corp., Madison, Wisc., for providing the aluminum billet for the welding experiments; Y. A. Chang of University of Wisconsin-Madison for letting us use the database required for calculating the T-f_S curves; Bruce Albrecht and Todd Holverson of Miller Electric Manufacturing Co., Appleton, Wisc., for donating the welding equipment (including Invision 456P power source, and XR-M wire feeder and gun); and the reviewers for their helpful comments.

References

1. Kou S. 2003. *Welding Metallurgy*, 2nd edition. pp. 103–114, 151, and 303–339. New York, N.Y.: John Wiley and Sons.

2. Dudas J. H., and Collins, F. R. 1966. Preventing weld cracks in high-strength aluminum alloys. *Welding Journal* 45(6): 241-s to 249-s.

3. Metzger, G. E. 1967. Some mechanical properties of welds in 6061 aluminum alloy sheet. *Welding Journal* 46(10): 457-s to 469-s.

4. Steenbergen, J. E., and Thornton, H. R. 1970. Quantitative determination of the conditions for hot cracking during welding for aluminum alloys. *Welding Journal* 49(2): 61-s to 68-s.

5. Gittos, N. F., and Scott, M. H. 1981. Heat-affected zone cracking of Al-Mg-Si alloys. *Welding Journal* 60(6): 95-s to 103-s.

6. Ma, T., and Den Ouden, G. 1999. Liquation cracking susceptibility of Al-Zn-Mg alloys.

International Journal for the Joining of Materials (Denmark) 11(3): 61–67.

7. Katoh, M., and Kerr, H. W. 1987. Investigation of heat-affected zone cracking of GTA welds of Al-Mg-Si alloys using the Varestraint test. *Welding Journal* 66(12): 360-s to 368-s.

8. Kerr, H. W., and Katoh, M. 1987. Investigation of heat-affected zone cracking of GMA welds of Al-Mg-Si alloys using the Varestraint test. *Welding Journal* 66(9): 251-s to 259-s.

9. Miyazaki, M., Nishio, K., Katoh, M., Mukae, S., and Kerr, H. W. 1990. Quantitative investigation of heat-affected zone cracking in aluminum Alloy 6061. *Welding Journal* 69(9): 362-s to 371-s.

10. Gitter, R., Maier, J., Muller, W., and Schwellinger, P. 1992. Formation and effect of grain boundary openings in AlMgSi alloys caused by welding. *Proceedings of 5th International Conference on Aluminum Weldments.* P. 4.1.1. D. Kosteas, R. Ondra, and F. Ostermann, ed. Technische Universita Munchen, Munich, Germany.

11. Powell, G. L. F., Baughn, K., Ahmed, N., Dalton, J. W., and Robinson, P. 1995. The cracking of 6000 series aluminum alloys during welding. *Proceedings of International Conference on Materials in Welding and Joining.* Institute of Metals and Materials Australasia, Parkville, Victoria, Australia.

12. Ellis, M. B. D., Gittos, M. F., and Hadley, I. 1997. Significance of liquation cracks in thick section Al-Mg-Si alloy plate. *The Welding Institute Journal* (UK) 6(2): 213–255.

13. Schillinger, D. E., Betz, I. G., Hussey, F. W., and Markus, H. 1963. Improving weld strength in 2000 series aluminum alloys. *Welding Journal* 42: 269-s to 275-s.

14. Young, J. G. 1968. BWRA experience in the welding of aluminum-zinc-magnesium alloys. *Welding Journal* 47(10): 451-s to 461-s.

15. Lippold, J. C., Nippes, E. F., and Savage, W. F. 1977. An investigation of hot cracking in 5083-O aluminum alloy weldments. *Welding Journal* 56(6): 171-s to 178-s.

16. Gutscher, D., and Cross, C. E. 2003. Effect of Cu and Fe on weldability of aluminum 2519. *Trends in Welding Research*, ASM International, Materials Park, Ohio, pp. 638–641.

17. Kou, S. 2003. Solidification and liquation cracking issues in welding. *JOM*, June, pp. 37–42.

18. Huang, C., and Kou, S. 2003. Liquation cracking in partial-penetration aluminum welds: Effect of penetration oscillation and backfilling. *Welding Journal* 82(7): 184-s to 194-s.

19. Huang, C., and Kou, S. 2004. Liquation cracking in full penetration Al-Cu Welds. *Welding Journal* 83(2): 50-s to 58-s.

20. Huang, C., and Kou, S. 2004. Liquation cracking in full penetration Al-Mg-Si welds. *Welding Journal* 83(4): 111-s to 122-s.

21. Huang, C., Cao, G., and Kou, S. 2004. Liquation cracking in partial-penetration aluminum welds: Assessing tendencies to liquate, crack and backfill. *Science and Technology of Welding and Joining*, vol. 9, pp. 1–9.

22. Huang, C., Kou, S., and Purins, J. R. 2001. Liquation, solidification, segregation and hot cracking in the partially melted zone of Al-4.5Cu welds. *Proceedings of Merton C. Flemings Symposium on Solidification Processing*. pp. 229–234. R. Abbaschian, H. Brody, and A. Mortensen, eds. The Mineral, Metals and Materials Society, Warrendale, Pa.

23. Flemings, M. C. 1974. *Solidification Processing.* pp. 34–36, 160–162, 256–258, and Appendix B. New York, N.Y.: McGraw-Hill.

24. Hatch, J. E. 1984. *Aluminum — Properties and Physical Metallurgy*, pp. 322–323, 338. Materials Park, Ohio: ASM International.

25. Borland J. C., and Rogerson, J. H. 1963. Examination of the patch test for assessing hot cracking tendencies of weld metal. *British Welding Journal* 8: 494–499.

26. Nelson, T. W., Lippold, J. C., Lin, W., and Baeslack III, W. A. 1997. Evaluation of the circular patch test for assessing weld solidification cracking, 1. Development of a test method. *Welding Journal* 76(3): 110-s to 119-s.

27. Houldcroft, R. T. 1954. Dilution and uniformity in aluminum alloy weld beads. *British Welding Journal* 1: 468–472.

28. *Binary Alloy Phase Diagrams. 1986.* vol. 1, p. 165, Materials Park, Ohio: ASM Int'l.

29. *Pandat* 2001. Phase diagram calculation software package for multicomponent systems, Computherm LLC, Madison, Wisc.

30. *PanAluminium* 2001. Thermodynamic database for commercial aluminum alloys, Computherm LLC, Madison, Wisc.

31. Liu, Z. K., and Chang, Y. A. 1999. Thermodynamic assessment of the Al-Fe-Si system. *Metallurgical and Materials Transactions* A 30A(4): 1081–1095A.

32. Liang, H., and Chang, Y. A. 1999. A thermodynamic database on aluminum alloys for practical alloy design. *Light Metals, Minerals, Metals and Materials Society*/AIME, pp. 875–881.

33. Chang, Y. A., Xie, F. Y., Kraft, T., Zuo, Y., and Moon, C. H. 1999. Microstructure and microsegregation in Al-rich Al-Cu-Mg alloys. *Acta Materialia* 47(2): 489–500.

34. Huang, W., and Chang, Y. A. 1998. A thermodynamic analysis of the Al-Re system. *Journal of Phase Equilibria* 19(4): 361–366.

35. Liang, H., and Chang, Y. A. 1998. A thermodynamic description for the Al-Cu-Zn system. *Journal of Phase Equilibria* 19(1): 25–37.

36. Liang, H., Chen, S. L., and Chang, Y. A. 1997. A thermodynamic description of the Al-Mg-Zn system. *Metallurgical and Materials Transactions* A 28A(9): 1725–1734A.

37. Chen, S. L., Zuo, Y., Liang, H., and Chang, Y. A. 1997. A thermodynamic description for the ternary Al-Mg-Cu system. *Metallurgical and Materials Transactions* A, 28A(2): 435–446A.

38. Zuo, Y., Chang, Y. A. 1996. Calculation of phase diagram and solidification paths of ternary. *Materials Science Forum* 215-216: 141–148.

39. Chang, Y. A., Chen, S. L., Zuo, Y., Zhang, F., Daniel, S. L., Moon, C. H. Liang, H., Xie, F. Y., Huang, W., and Liu, Z. K. 1996. Phase diagram calculation: a critical tool for alloy and processing design. *Proceedings of The International Conference-MSMM'96. Modeling and Simulation in Metallurgical Engineering and Materials Science*, pp.185–190, Metallurgical Industry Press.

40. Chen, S. L., and Chang, Y. A. 1993. A thermodynamic analysis of the Al-Zn system and phase diagram calculation. *Calphad* 17(2): 113–124.

41. Zuo, Y., and Chang, Y. A. 1993. Thermodynamic calculation of the aluminum-magnesium phase diagram. *Calphad* 17(2): 161–174.

42. Zuo, Y., Chang, Y. A. 1992. Calculation of phase diagram and solidification paths of aluminum-rich Al-Mg-Cu ternary alloys. *The Minerals, Metals & Materials Society*, pp. 935–942.

43. Chen, S. W., Beumler, H. W., and A. Chang, Y. 1991. Experimental determination of the phase equilibria of aluminum-rich Al-Li-Cu alloys. *Metallurgical Transactions* A 22A(1): 203–213.

44. Chen, S. W., and Chang, Y. A. 1991. Application of thermodynamic models to the calculation of solidification paths of aluminum-rich Al-Li alloys. *Metallurgical Transactions* A 22A(1): 267–271.

45. Chen, S. W., Lin, J. C., Chang, Y. A., and Chu, M. G. 1990. Phase equilibria and solidification of aluminum-rich Al-Li-Cu alloys. *The Minerals, Metals & Materials Society*, pp. 985–988.

46. Chen, S. W., Jan, C. H., Lin, J. C., and Chang, Y. A. 1989. Phase equilibria of the Al-Li binary system. *Metallurgical Transactions* A 20A(11): 2247–2258.

47. Chen, S. W., Chang, Y. A., and Chu, M. G. 1989. Phase equilibria and solidification of Al-Li alloys. *Materials and Component Engineering Publications* Ltd., pp. 585–594.

48. Singer, A. R. E., and Cottrell, S. A. 1946. Properties of the Al-Si alloys at temperatures in the region of the solidus. *Journal of Institute of Metals* 73: 33–54.

49. Pumphrey, W. I., and Jennings, P. H. 1948. High-temperature tensile properties of cast aluminum-silicon alloys and their constitutional significance. *Journal of Institutive of Metals*, 74: 203–233.

50. Dahle, A. K., and Arnberg, L. 1997. Development of strength in solidifying aluminum alloys. *Acta Materialia*, 45: 547–559.

51. Arnberg, L., Chaii, G., and Backerud, L. 1993. Determination of dendritic coherency in solidifying melts by rheological measurements. *Materials Science and Engineering*, A173: 101–103.

52. The Aluminum Association. 1982. *Aluminum Standards and Data.* p. 203, Washington, D.C.: The Aluminum Association.